Molecular Origins of Dye Aggregation and Complex Formation Effects in Coumarin 343

ARTICLE *in* THE JOURNAL OF PHYSICAL CHEMISTRY C · JUNE 2013

Impact Factor: 4.77 · DOI: 10.1021/jp4024266

THE JOURNAL OF PHYSICAL CHEMISTRY C

Article

pubs.acs.org/JPCC

Molecular Origins of Dye Aggregation and Complex Formation Effects in Coumarin 343

Xiaogang Liu,[†] Jacqueline M. Cole,*[,†,‡,§] and Kian Sing Low[†]

[†]Cavendish Laboratory, Department of Physics, University of Cambridge, J. J. Thomson Avenue, Cambridge, CB3 0HE United Kingdom

[‡]Department of Chemistry, University of New Brunswick, P.O. Box 4400, Fredericton, NB, E3B 5A3 Canada

[§]Department of Physics, University of New Brunswick, P.O. Box 4400, Fredericton, NB, E3B 5A3 Canada

ABSTRACT: Solvent effects have a significant impact upon the optoelectronic properties of coumarin 343, which are mainly exploited in the solution phase for a diverse range of applications, including lasers and dye-sensitized solar cells. The influence of solvation on the structure−property relationships for coumarin 343 are analyzed herein using (time-dependent) density functional theory (DFT/TD-DFT) based quantum calculations, in conjunction with UV−vis absorption and ^{1}H NMR spectroscopic measurements. Specifically, these solvent effects on the peak UV−vis absorption wavelengths (λ_{max}^{abs}), and molecular geometry changes of coumarin 343 are investigated. Coumarin 343 is shown to be prone to dye aggregation; its different molecular aggregation phases, UV−vis absorption profiles, and formation mechanisms are discussed using three representative solvents: cyclohexane [nonpolar and non-hydrogen bonding (NHB)], benzene (polar and nearly NHB), and ethanol (polar and hydrogen-bond accepting/donating). It is also demonstrated that the intramolecular hydrogen bond in coumarin 343 can be "opened up" in hydrogen-bond accepting solvents. Furthermore, this study elucidates the solvent effects on the molecular conformations of coumarin 343. The much deeper understanding of the molecular aggregation and complex formation mechanisms in coumarin 343 provides key building blocks for the knowledge-based molecular design of coumarin dyes with antiaggregation characteristics. The associated molecular engineering prospects for these dyes stand to improve device performance for optoelectronic applications.

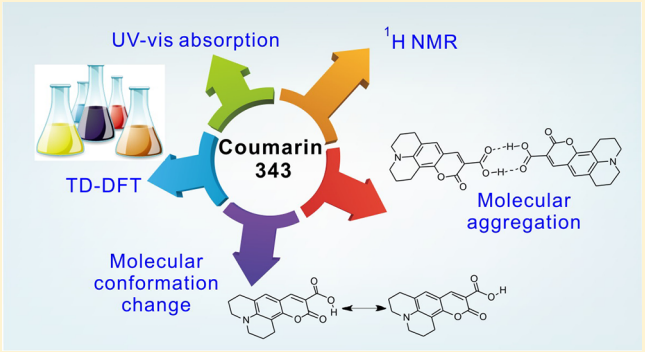

1. INTRODUCTION

Coumarin 343 (**1**; alternative name: coumarin 519; $C_{16}H_{15}NO_4$; Scheme 1) is a popular dye used in many different applications, such as solution dynamic probes,[1] laser dyes,[2] and, more recently, organic sensitizers in dye-sensitized solar cells (DSC).[3] Since the functionality of this coumarin is exploited largely in the solution phase, understanding its behavior in different solvents is essential in order to facilitate its widespread application. Nevertheless, the photophysics and photochemistry of this dye in the solution phase is much more complicated than those of many other coumarin derivatives. For example, its peak UV−vis absorption wavelength (λ_{max}^{abs}) in ethanol has been reported at 425,[4] 434.9,[1a] 439,[5] 442,[6] 446,[7] and 449 nm.[8] This range of 24 nm is significantly beyond typical systematic differences between UV−vis spectroscopy instruments, and such inconsistent data clearly suggest some unusual behavior of **1**. A thorough understanding of the exact structure of **1** in its solvated phase and its associated properties is therefore crucial for optimizing its prevalent application.

Density functional theory (DFT) and time-dependent density functional theory (TD-DFT) turn out to be powerful tools to model coumarins both in the gas phase and in solution.[9] With DFT/TD-DFT calculations, one can determine the most stable coumarin structures in different media, as well as their UV−vis absorption/fluorescence profiles. For example, comprehensive studies on the energetic stabilities for various conformational isomers of **1** have been conducted by Cave et

Scheme 1. Conformational Isomers of 1 (A—D and a—f) and Its Deprotonated Form (g)

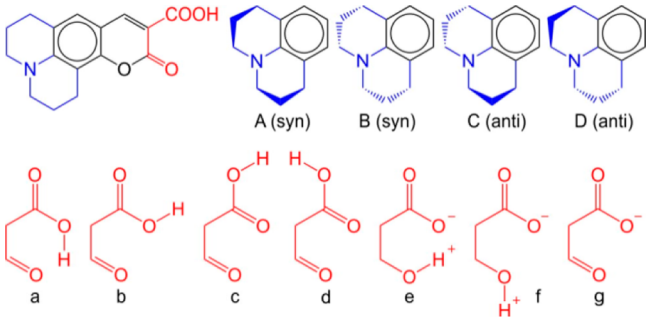

Received: March 9, 2013
Revised: May 19, 2013
Published: June 18, 2013

dx.doi.org/10.1021/jp4024266 | J. Phys. Chem. C 2013, 117, 14723−14730

al. and Wu et al.[9a,b] Four types of isomers of the julolidyl moiety of **1** have been considered (Scheme 1A—D). The pairs of syn structures (A and B) and two anti structures (C and D) are isoenergetic, respectively, as they are mirror images of each other with respect to the plane defined by the coumarin framework (Scheme 1; highlighted in black). Furthermore, it has been found that the syn structures are the most stable configurations in the gas phase, versus the anti structures in solution. Nevertheless, the energy differences among these julolidyl isomers are within 0.010 eV of each other, much smaller than thermal energy at 300 K ($1.5kT \approx 0.039$ eV). Therefore, a coexistence of all four types of julolidyl structures is expected at room temperature. Since the focus of this paper is on solution properties, where the anti structure has the lower conformation energy, all of our calculations on **1** will henceforth be based on the anti structure C. In contrast, considerable energy differences are invoked by the different geometries associated with the −COOH group. In total, six isomers (Scheme 1a—f) of this functional group have been analyzed. The most stable geometry forms an intramolecular hydrogen bond with the carbonyl oxygen (Scheme 1a). The energy of the next two most stable conformations is 0.255 and 0.312 eV higher than the global minimum, respectively (Scheme 1b,c). Wu et al. also considered the presence of a deprotonated structure of **1** (Scheme 1g) in methanol. It was concluded that, in pure methanol, the deprotonated structure is not likely to occur, based on a comparison of the measured and calculated λ_{max}^{abs} for both neutral and deprotonated **1**.

However, it should be pointed out that solvent effects are often classified into two categories, namely, nonspecific solvent effects and specific solvent effects.[10] By a nonspecific solvent effect, we mean that the solvent acts as a continuous and uniform dielectric. In contrast, specific solvent effects concern a directional, nonuniform distribution of the molecular-level interactions between solvents and solutes, such as hydrogen bond interactions, probe−probe interactions (i.e., forming excited dimers), and acid−base chemistry (electron-pair donor/electron-pair acceptor interactions).[10,11] It has been demonstrated that specific solvent effects play an important role in the solvatochromism of coumarins.[12] On the contrary, previous computational studies only take into account nonspecific solvent effects, ignoring the specific solvent effects on the molecular conformations of **1**; such treatments may potentially bias the results.

In this paper, UV−vis absorption and ^{1}H NMR spectroscopic measurements, and more thorough DFT/TD-DFT calculations are performed on **1**, in order to comprehend the nature of its exact structures when in solution. It will be shown that the intramolecular hydrogen bond in **1** can be "opened up" in hydrogen bond accepting (HBA) solvents. Furthermore, **1** presents a strong tendency to form dimers and/or high-order molecular aggregates in a wide range of solvents, even at low concentrations; and the anomalous UV−vis absorption/fluorescence profiles and numerous inconsistent λ_{max}^{abs} values in the literature can be explained by dye aggregation. These aggregates render the dye undesirable for many applications, such as in dye lasers and DSCs. This finding is therefore highly relevant to the optoelectronic applications involving **1** and other similar chemicals.

2. EXPERIMENTAL AND COMPUTATIONAL METHODS

2.1. Solution-State UV−vis Absorption Spectroscopy. Compound **1** was supplied by Exciton and used without further purification. Dilute solution samples (with absorption below 10% of the incident light) in cyclohexane, toluene, toluene/*n*-pentane (10:90) mixture, and ethanol were tested on a Hewlett-Packard G1103A spectrophotometer. The uncertainties in all λ_{max}^{abs} readings are ±1 nm.

2.2. Solution-State ^{1}H Nuclear Magnetic Resonance (NMR) Spectroscopy. For ^{1}H NMR spectroscopy experiments, **1** was dissolved into deuterated dimethyl sulfoxide (DMSO) in a high concentration of 9.3×10^{-3} M. The NMR spectra of this sample were collected using a Bruker Avance 500 Cryo Ultrashield NMR spectrometer at five different temperatures: 298, 303, 308, 313, and 318 K. Chemical shifts were measured relative to those of an internal tetramethylsilane reference.

2.3. DFT and TD-DFT Calculations. Quantum-chemical calculations were performed on **1** using *Gaussian 09*.[13] Becke's three-parameter and Lee−Yang−Parr hybrid functional (B3LYP)[14] was used in all calculations, and the basis sets in use were adjusted accordingly as the computational load became heavier.

The geometries of the monomers of **1** (Scheme 1a—c) were optimized using B3LYP/6-311++G(2d,2p) in vacuo and in ethanol and DMSO.[15] The geometries of dimers and trimers of **1** were optimized in vacuo with the counterpoise correction[16] using B3LYP/6-31G(d).[17] The geometries of dimers were also optimized using B3LYP/6-31+G(d,p)[17] without a counterpoise correction in vacuo, and in cyclohexane, benzene and ethanol, as this correction is not currently supported when solvent effects are included. In order to study the interaction of **1** with ethanol/DMSO, the complexes formed by **1** coupling with an ethanol/DMSO molecule in different configurations were optimized in ethanol/DMSO using B3LYP/6-31+G(d,p). Following this, TD-DFT calculations were carried out on the monomers and dimers of **1** in cyclohexane, benzene, and ethanol using B3LYP/6-31+G(d,p), in order to determine their peak absorption wavelengths.

In all calculations, frequency checks were performed after each geometry optimization in order to ensure that minima on the potential energy surfaces were found and all solvent effects were incorporated via the polarizable continuum model (PCM).[18]

3. RESULTS AND DISCUSSION

3.1. Molecular Aggregation of 1. It will herein be demonstrated that a substantial part of the disparity in literature λ_{max}^{abs} values of **1** can be attributed to its molecular aggregation, even at low concentrations. The relative energetic stability between monomers and molecular aggregates of **1** is therein assessed.

In this study, molecular aggregates of **1** are broadly classified into two types: low-order and high-order aggregates. For low-order aggregates, several molecules of **1** are connected together in a head-to-head fashion via intermolecular hydrogen bonds between their −COOH groups (Figure 1a,b). Both dimers and trimers of conformational isomers **b** and **c** (Scheme 1) belong to this type. The high-order aggregates, known as "J-type" aggregates,[19] are formed via the head-to-tail connection of multiple molecules. While the exact structure of the high-order aggregate is not known, the crystal structure of **1** provides a first-order approximation (Figure 1c).[20] The energy of high-order aggregates depends on their size, and is not calculated. Nevertheless, since high-order aggregates start to appear when

dx.doi.org/10.1021/jp4024266 | J. Phys. Chem. C 2013, 117, 14723−14730

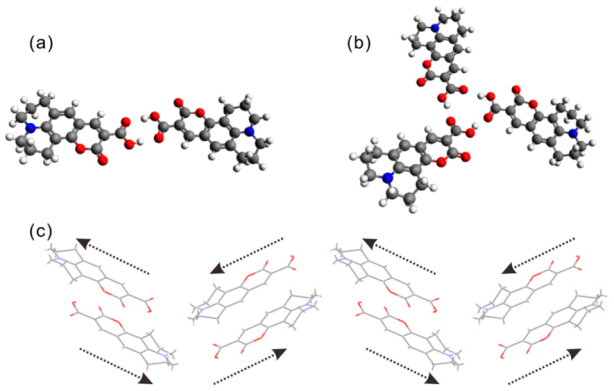

Figure 1. (a) Dimer model of **1**. (b) Trimer model of **1**; only the dimer and the trimer formed by conformational isomer **b** of **1** are shown here, while those by isomer **c** have similar configurations and are also considered in our analysis. (c) A high-order aggregate; a cluster of eight molecules extracted from the crystal structure of **1**, representing a first-order approximation to the high-order aggregate in solution. The arrows indicate the dipole moment of **1**.

the concentration of **1** rises above a certain threshold, they should have relatively low energy at high concentrations of **1**.

The energy of three monomers, two dimers and two trimers in vacuo were computed using *Gaussian 09* (Figure 2). Monomers **a**, **b**, and **c** represent the three most stable conformational isomers of **1**.[9a] In particular, results show that **a** is the lowest energy monomer; this finding can be attributed to its ability to form an intramolecular hydrogen bond. Because of this hydrogen bond, monomer **a** does not have a potential to form dimers and trimers. On the contrary, both **b** and **c** are able to create dimers (for example, **b**-**b** and **c**-**c**; Figure 2) and trimers (for example, **b**-**b**-**b** and **c**-**c**-**c**; Figure 2), which are energetically stabilized via intermolecular hydrogen bonds. Despite the fact that monomers **b** and **c** are less stable than **a**, the computational results demonstrate that their dimers and trimers possess even lower energies than monomer **a** in vacuo (Figure 2). Furthermore, dimers are thermodynamically more stable than trimers (and tetramers and so forth as expected; Figure 2); kinetically, dimers are also more favorable, as only two molecules of **1** are required for its formation. Therefore, dimers are considered to be preponderant among all low-order aggregates.

The energetic stability of dimers with respect to monomers, however, decreases as the solvent polarity rises. This is a result of larger dipole moments of monomers compared to the (nearly) zero dipole moments of low-order aggregates. Consequently, monomers experience a greater energy reduction through solvent stabilization. This effect becomes more apparent as solvent polarity increases, as reflected by the relative energy differences of monomer **a**, dimer **b**-**b**, and dimer **c**-**c** in four different media: vacuum (dielectric constant $\varepsilon_r = 0$), cyclohexane ($\varepsilon_r = 2.0165$), benzene ($\varepsilon_r = 2.2706$), and ethanol ($\varepsilon_r = 24.852$; Figure 3).

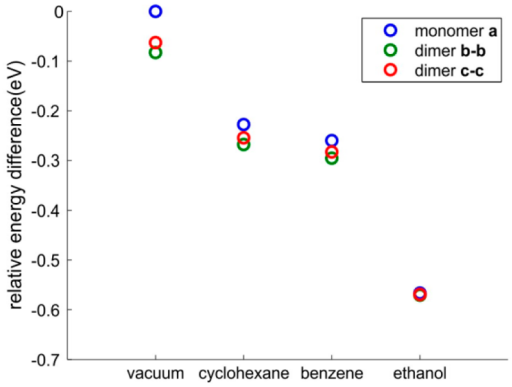

Figure 3. Relative energy differences among monomer **a** and dimers **b**-**b** and **c**-**c** in four different media. Their energy differences are evaluated by their optimized structures at the B3LYP/6-31+G(d,p) level. The solvent effect is modeled by PCM; no counterpoise correction is performed in these calculations for consistency, as this function is not supported in the PCM within *Gaussian 09*.

It should be highlighted that the actual energy of **a** in benzene ($\alpha = 0$, and $\beta = 0.10$) and ethanol ($\alpha = 0.86$, and $\beta = 0.75$) should be even lower, due to the stabilization effect from the specific solvent interactions. Here α, β, as well as π^* are three solvent property scales defined in the Taft-Kamlet solvatochromic comparison method.[21] In this model, π^* describes the solvent polarity (which refers to dipolarity and polarizability jointly); α refers to solvent hydrogen-bond donor (HDB) acidity (the ability of the solvent to donate a proton to a solvent-to-solute hydrogen bond), and β relates to the solvent hydrogen-bond acceptor (HBA) basicity (the ability of the solvent to accept a proton from a solvent-to-solute hydrogen bond). These three parameters collectively describe the strength of a particular solvent in contributing to various solvent effects. The nonzero values of α and/or β in benzene

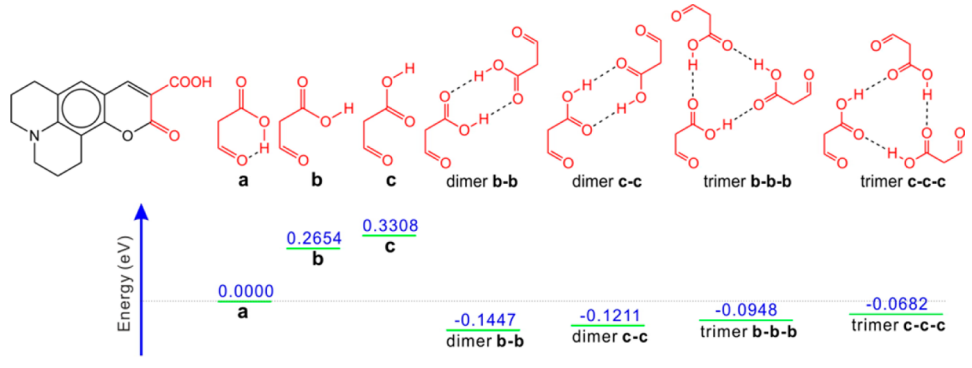

Figure 2. Conformational isomers of **1**, its low-order aggregates, and their corresponding energy in vacuo (eV). The energy differences between monomers are calculated based on their optimized structures at the B3LYP/6-311++G(2d,2p) level; the relative energy of the low-order aggregates with respect to the monomer **a** are computed at the B3LYP/6-31G(d) level with counterpoise corrections using *Gaussian 09*.

dx.doi.org/10.1021/jp4024266 | *J. Phys. Chem. C* 2013, 117, 14723−14730

Table 1. Two Solution Preparation Methods for 1 in Cyclohexane Solvent

method A	method B
1. Add **1** directly into cyclohexane. Due to its low solubility, saturated cyclohexane solution and precipitates of **1** are formed.	1. Add a known amount of **1** into acetonitrile. Compound **1** has high solubility in this solvent.
2. Take the saturated solution and dilute it to different ratios with more cyclohexane.	2. Take a small amount of the prepared acetonitrile solution and add it into cyclohexane in order to achieve the required concentration.
	3. Bubble nitrogen gas until acetonitrile evaporates from the cyclohexane solution.

and ethanol indicate that the specific interactions via hydrogen bonds are present in these two solvents. However, such effects are not taken into account in the PCM. For dimers **b-b** and **c-c**, this specific solvent effect should be rather weak. This is because their −COOH groups participate in intermolecular hydrogen bonds and the interactions with solvents are thus minimized. However, the specific solvent effect in vacuo and in cyclohexane ($\alpha = \beta = 0$) is not relevant to either monomers or dimers.

Next, the presence of different types of molecular aggregate and their formation mechanisms are analyzed in three representative solvents: cyclohexane [nonpolar and non-hydrogen bonding (NHB)], benzene (polar and nearly NHB), and ethanol [polar and hydrogen bond accepting/donating (HBA/D)].

3.1.1. Molecular Aggregates of 1 in a Nonpolar and NHB Solvent (Cyclohexane). The complexity of molecular aggregation of **1** in cyclohexane is probably best illustrated via a comparison of its UV−vis absorption profiles, where solutions of **1** were prepared by two different methods (Table 1); while they comprise the same solute, the same solvent, the same temperature and the same (apparent) concentration. Yet, their λ_{max}^{abs} values are different; unexplained overall red shifts are noted, and the relative intensities of different peaks vary (Figure 4). Upon close inspection, molecular aggregation appears to be the cause of these discrepancies.

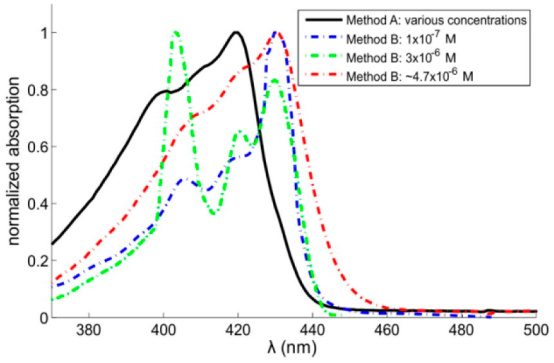

Figure 4. UV−vis absorption profiles of **1** in cyclohexane. The solutions are prepared via two different methods (Table 1). Data of the green and blue spectra are retrieved from the work of Correa et al.,[1a] since our UV−vis absorption spectroscopy apparatus has limited dynamic range and cannot detect the signal in very dilute solutions.

For the solution prepared via method A (Table 1), the peak absorption lies at 419 nm, while there are hints of two further unresolved peaks in the range of 398—402 and 410−412 nm. This profile remains almost unchanged as the solution is diluted to different ratios. Note that the dissolution of **1** directly into cyclohexane is a very slow process, taking ∼10 h to reach equilibrium at room temperature.

For the solution obtained via method B (Table 1), however, there are three distinct peaks, at 406, 419, and 430 nm, respectively; and the relative weights of these three peaks vary, as the concentration of **1** increases. At low concentration (1×10^{-7} M), the peak at 406 nm is the strongest; at high concentration (3×10^{-6} M and above), the peak at 430 nm becomes the most significant. Nevertheless, all three peaks are discernible at these concentrations.

Both solutions prepared via methods A and B remain stable indefinitely at room temperature. When they were tested over a time period of one month, no change in the UV−vis absorption profiles was noticed.

Correa and co-workers have assigned the peaks at 406 and 430 nm to monomers and high-order aggregates of **1**, respectively, via an excellent study on the absorption and fluorescence of **1** in cyclohexane.[1a] (In their paper, the latter peak is reported at 425 nm; however, a closer look at their data suggests that this peak is actually located at 430 nm.) However, in their experiment, a peak at 419 nm was relatively weak and not assigned. Method B had been used to prepare solutions;[22] this peak becomes notable when the solution is prepared via method A.

We attribute the peak at 419 nm to dimers of **1** as a result of our TD-DFT calculations (Table 2). The theoretical calculations successfully reproduce the red shift of λ_{max}^{abs} values as solvent polarity increases, and further predict the relative red shift of dimers with respect to monomers. Since the peak of **1** at 419 nm also demonstrates a similar bathochromic shift with respect to that of monomers at 406 nm, it is reasonable to assign this peak to dimers. The formation of dimers for other carboxylic acids in nonpolar solvents has been reported previously.[23]

Different molecular aggregation mechanisms of **1** in cyclohexane via both methods A and B are also proposed to explain the discrepancy between UV−vis absorption profiles. In cyclohexane, the dimers are more stable than monomers (Figure 3). Hence, directly dissolving **1** into cyclohexane via method A leads to a preponderance of dimers. These dimers are resistant to high-order aggregation. The switching from one to the other must go through a high energy barrier, as a result of the relative competition between their head-to-head connections versus the head-to-tail connection in high-order aggregates. Furthermore, the formation of dimers involves the "opening up" of the intramolecular hydrogen bonds of monomers **a**. This "opening up" process can be assisted by HBA solvents. Nevertheless, it is purely thermally activated in NHB cyclohexane. This explains why the dissolution of **1** into cyclohexane is a very slow process. Lastly, it is interesting to note that the formation of dimers enhances the solubility of **1** in cyclohexane. Compound **1** is polar and has very low solubility in nonpolar solvents. Yet, by forming a dimer, its centrosymmetry results in a net reduction of the dipole moment of **1** to zero. This greatly facilitates the solubility of **1** in cyclohexane, up to $\sim 2.3 \times 10^{-5}$ M. Similarly, although **1** is practically insoluble in *n*-pentane, forming dimers drives up its solubility to $\sim 7.9 \times 10^{-6}$ M.

dx.doi.org/10.1021/jp4024266 | J. Phys. Chem. C 2013, 117, 14723−14730

Table 2. Theoretical and Experimental λ_{max}^{abs} Values (nm) of the Monomers, Dimers, and High-Order Aggregates of 1[a]

		theoretical (PCM)			experimental[b]		
solvent	dielectric constant	monomer **a**	dimer **b-b**	dimer **c-c**	monomers	dimers	high-order aggregates
cyclohexane	2.0165	395.01	401.93	401.02	406	419	430
benzene	2.2706	397.93	404.38	403.46	418		442
ethanol	24.852	405.25	416.41	415.80	436		444

[a]Overall, the theoretical values show a decent match to experimental data, and successfully reproduce the red shift of λ_{max}^{abs} as solvent polarity increases. The theoretical calculations also predict the relative red shift of dimers with respect to monomers. In addition, there are slight underestimations of λ_{max}^{abs} values in our calculation, and the errors tend to grow as the solvent is changed from cyclohexane to benzene/ethanol. This is largely because the specific solvent effect for benzene and ethanol has been ignored in the PCM, while this effect is absent in cyclohexane. [b]The experimental λ_{max}^{abs} values of monomers and high-order aggregates in benzene were imported from the literature,[1] while the results in the rest solvents were from our in-house measurements.

Using method B, compound **1** is first dissolved into acetonitrile. In this solvent (ε_r = 35.688), the monomers have lower energy than dimers. Hence, monomers and high-order aggregates (at relatively high concentrations) are more stable. These states are also largely preserved when this solution is transferred into cyclohexane, due to the energy barrier associated with switching to dimers. In addition, when in a mixture of acetonitrile and cyclohexane, **1** prefers to associate with polar acetonitrile molecules. As acetonitrile evaporates from the solution, however, the molecules of **1** are compressed into a smaller domain of acetonitrile. This leads to the enhancement of the high-order aggregates; this effect becomes more noticeable, when a larger quantity of **1** in acetonitrile is added into cyclohexane. Therefore, the dominant peak of **1** alters from 406 nm (monomers) to 430 nm (high-order aggregates) as its concentration rises in cyclohexane.

3.1.2. Molecular Aggregates of 1 in a Polar and (Nearly) NHB Solvent (Benzene and Benzene/n-Heptane Mixture). Gutierrez and co-workers have reported an interesting study on the UV−vis absorption spectra of **1** in benzene and benzene/*n*-heptane.[1b] They concluded that the equilibrium between monomers and dimers of **1** shifts toward monomers as the solvent polarity decreases. Their conclusion is in contrast to our DFT calculation results (Figure 3), which suggests that the dimers, not monomers, are more stable in less polar solvents. We respectfully disagree with their assertion, and will justify ours using both their experimental data and our in-house measurements.

First, the spectra of **1** in a benzene/*n*-heptane (10:90) mixture needs to be considered, as its solvent properties ($\pi^* \approx 0.02$, $\alpha \approx 0$ and $\beta \approx 0.01$)[24] are very close to those of cyclohexane ($\pi^* = \alpha = \beta = 0$).[25] In this mixed solvent solution, the UV−vis absorption profile bears two peaks, located at 408 and 430 nm, according to Gutierrez et al. (Figure 5a).[1b] They assigned these two peaks to the monomers and dimers of **1**, respectively. We argue that the peak at 430 nm actually corresponds to high-order aggregates, but not dimers, for the following three reasons: (1) the benzene/*n*-heptane (10:90) mixture and cyclohexane have very similar solvent properties; the absorption peaks of **1** in these two solvents should therefore be very close to each other. For example, the monomers absorb maximally at 408 nm in the mixture and 406 nm in cyclohexane. (2) By the same token, the 430 nm peak in the benzene/*n*-heptane (10:90) mixture is more likely to be caused by high-order aggregates, because the absorption of these aggregates peaks at 430 nm in cyclohexane, cf. 419 nm for dimers. (3) Dimers usually afford a strong ^{1}H NMR chemical shift in the range of δ = 10—13.2.[23] Yet, Gutierrez et al.[1b] did not observe any corresponding ^{1}H NMR signal for **1** in the benzene/*n*-heptane (10:90) mixed solvent with λ_{max}^{abs} at 430 nm.

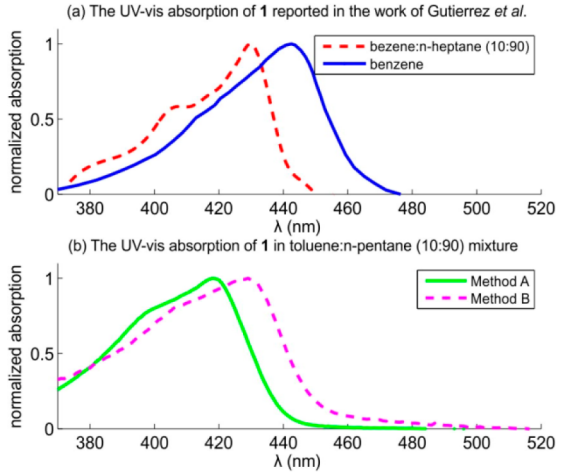

Figure 5. UV−vis absorption profiles of **1**: (a) in benzene and bezene/*n*-heptane mixture; (b) in toluene/*n*-pentane mixture.

The fact that Gutierrez et al.[1b] did not observe dimers is assumed to be related to their solution preparation method. To verify this assumption, a solution of **1** in a toluene/*n*-pentane (10:90) mixture ($\pi^* \approx -0.02$, $\alpha \approx 0$ and $\beta \approx 0.01$)[24] was prepared in house using both methods A and B (Table 1). Toluene and *n*-pentane are very similar solvents to benzene and *n*-heptane, respectively, and were more readily available. According to this experiment, dimers prevail in the solution prepared via method A, while high-order aggregates form via method B, as in cyclohexane ([Figure 5b).

As the benzene content of the benzene/*n*-heptane mixture increases, the UV−vis absorption peak, due to high-order aggregates, gradually shifts from 430 to 442 nm in pure benzene. In contrast, Gutierrez et al.[1b] have attributed the peak at 442 nm to dimers in benzene. This mis-assignment eventually leads to their dubious conclusion on the relative stability between monomers and dimers.

In fact, with **1** in a benzene/*n*-heptane mixture, as the content of benzene rises and the solvent polarity increases, the energy of both monomers and dimers decreases due to a progressively greater solvent stabilization effect. However, the energy reduction is more significant for monomers, owing to their large dipole moments. Therefore, the equilibrium between monomers and dimers shifts toward monomers in more polar solvents and dimers are less stable in polar solvents. For instance, when the toluene solution of **1** was prepared by method A, a peak due to high-order aggregates was observed

dx.doi.org/10.1021/jp4024266 | J. Phys. Chem. C 2013, 117, 14723−14730

and a clear peak due to dimers was absent, unlike that in cyclohexane. Preparing the solution by method B produces the same high-order aggregate peak but no dimer peak.

3.1.3. Molecular Aggregates of 1 in a Polar and HBD/A Solvent (Ethanol). Dimers of **1** are less polar than monomers. In polar solvents, such as ethanol, dimers are less stable than monomers, due to relatively weaker dipole−dipole interactions with solvent molecules and smaller solvent stabilization effect (Figure 3). Indeed, our experiments show that dimers are not likely to form in these solvents, regardless of the solution preparation methods; and only monomers and high-order aggregates are present in polar solvents.

Moreover, monomers and high-order aggregates do not show distinct peaks in the solution of **1** in ethanol. This featureless profile is due to the strong interaction between **1** and ethanol, resulting in very broad absorption spectra. However, the development of high-order aggregates is still observable through the shift of λ_{max}^{abs} from 436 to 444 nm, as a function of increasing concentration of **1** from 2.40×10^{-7} to 1.67×10^{-5} M (Figure 6). This red shift indicates that the high-order

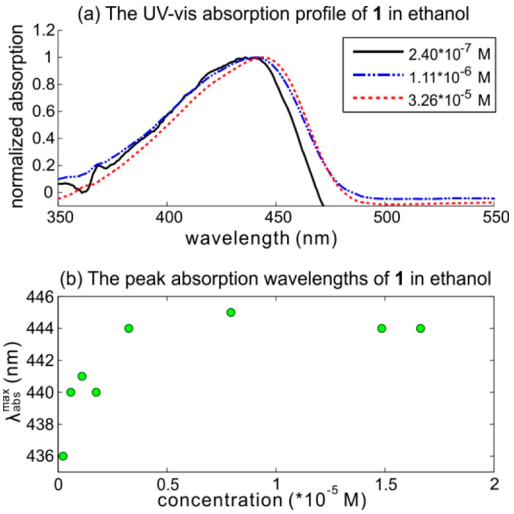

Figure 6. UV−vis absorption profiles of **1** in ethanol as a function of concentration.

aggregates are of J-type,[19,26] i.e., with a head-to-tail connection of multiple molecules (Figure 1c). Note that the absorption units of all these solutions are less than unity, which is expected of low concentrations. However, compound **1** is so prone to molecular aggregation that the aggregates start to form even at these reasonably low concentrations (5.80×10^{-7} to 1.67×10^{-5} M). This observation partially explains the large range of λ_{max}^{abs} values reported in the literature.

The root cause for the susceptibility of **1** to molecular aggregation is largely related to its planar molecular configuration, resulting in close packing and strong intermolecular interactions.[20] This effect is probably best illustrated by a comparison of the crystal packing in **1**, with that in coumarin 314T, which is another very similar coumarin derivative and yet is not vulnerable to molecular aggregation. Due to the planar geometry of **1**, the distance between two adjacent layers of molecules in the crystal of **1** is only 3.483 Å and there is a large overlap between them, resulting in relatively strong $\pi\cdots\pi$ interactions.[20] In contrast, with methyl groups on the julolidyl moiety, the interlayer distance in the crystal structure of coumarin 314T is significantly larger (4.331 Å), which effectively reduces its intermolecular interactions and prevents aggregation.[20]

3.2. Presence of Monomers in HBA Solvents. It has been suggested that the carboxylic acid groups in the monomers of **1** form intramolecular hydrogen bonds both in vacuo and in solution (Figure 2), based on theoretical calculations, using the PCM to emulate the solvent.[9a,b]

However, experimentally it has been shown that both the specific solvent effect, which concerns molecular-level interactions between **1** and solvent molecules, and the nonspecific solvent effect, which treats the solvent as a continuous dielectric medium, play important roles in the overall solvent effects on coumarins.[12a] Nevertheless, the PCM only takes into account the latter solvent effect, but ignores the former.

To take into account the specific solvent effect, DFT calculations on **1** were performed herein with the extra feature that a solvent molecule was placed explicitly near the H atom of the −COOH group of three most stable isomers of **1**, at a typical hydrogen-bond distance of ∼1.8 Å (Figure 7). This H

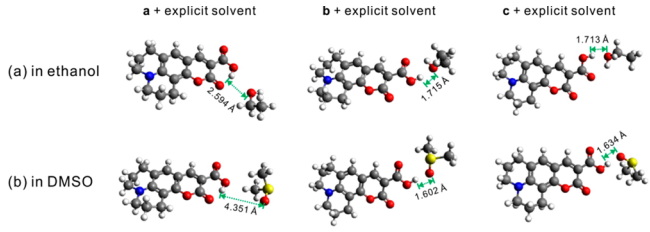

Figure 7. DFT optimized solution-state structures of isomers **a**—**c** calculated by explicit incorporation of a solvent molecule (a) ethanol and (b) DMSO.

placement is the only (significant) difference in the conformations of these three isomers. Note that we showed earlier that **a** has an intramolecular hydrogen bond, whereas isomers **b** and **c** do not (section 3.1).

Two standard HBA solvents, ethanol ($\pi^* = 0.540$, $\alpha = 0.860$, and $\beta = 0.750$) and DMSO ($\pi^* = 1.000$, $\alpha = 0$, and $\beta = 0.760$), were employed in this study. The geometries of three conformational isomers, **a**, **b**, and **c** of **1** and an ethanol/DMSO molecule were optimized using B3LYP/6-31+G(d,p) in order to study their interactions and evaluate their energy.

Results demonstrate that the interaction between the conformational isomer **a** of **1** and the explicitly placed solvent molecule (both ethanol and DMSO) is relatively weak, as their "hydrogen-bond" lengths increase significantly beyond typical values of ∼1.8 Å (Figure 7). This is because the H atom of the −COOH group in **1** participates in the intramolecular hydrogen bond, and its bond angle does not favor the formation of this intermolecular hydrogen bond with the explicit solvent molecule. In contrast, conformational isomers **b** and **c** of **1** are able to establish strong intermolecular hydrogen bonds with ethanol or DMSO molecules. As a result, a more significant energy reduction occurs for these two types of isomers such that they turn out to be energetically comparable to isomer **a** (Table 3).

This analysis suggests that the intramolecular hydrogen bond of **1** can be "opened up" in a HBA solvent. To corroborate this argument, we have performed ^{1}H NMR spectroscopy experiments on **1** in DMSO at different temperatures (Figure 8). Where a strong intramolecular hydrogen bond exists, the temperature drift of the NMR chemical shift for a carboxylic proton resonance is expected to lie in the range of ∼1—3 ppb/

dx.doi.org/10.1021/jp4024266 | J. Phys. Chem. C 2013, 117, 14723−14730

Table 3. Energy Differences (ΔE) between the Three Most Stable Isomers of 1 in Vacuo, in Ethanol, and in DMSO (eV)[a]

local environment of **1**	ΔE between isomers (relative to **a**)	
	isomer **b**	isomer **c**
vacuum	0.2654	0.3308
ethanol (PCM)	0.2658	0.2726
DMSO (PCM)	0.2524	0.2548
ethanol (explicit solvent molecule + PCM)	−0.0282	−0.0367
DMSO (explicit solvent molecule + PCM)	−0.0876	−0.0612

[a]The energy differences among these (isomer + ethanol/DMSO) complexes are evaluated based on the total energy of each complex.

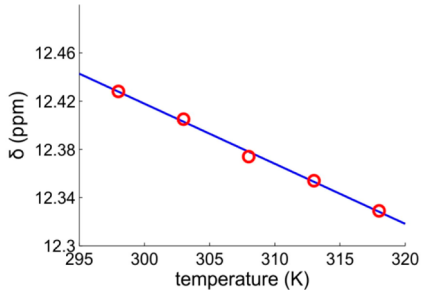

Figure 8. Temperature dependence of the ^{1}H NMR chemical shift δ (ppm) for the carboxylic proton resonance of **1** in DMSO. The best linear fit shows that the temperature coefficient is ~4.98 ppb/K.

K in DMSO, cf. greater values for intermolecular hydrogen bonds.[27] However, a relatively large temperature coefficient of 4.98 ppb/K was observed in our experiments. This large coefficient suggests that the intramolecular hydrogen bond in **1** has been "opened up" for at least a substantial number of monomers. In fact, similar hydrogen bond "opening up" mechanisms have been reported previously for a few benzotriazole compounds in DMSO.[28]

Lastly, in order to further support this finding, the temperature coefficient of the ^{1}H NMR chemical shift for the carboxylic proton of *para*-methyl red ($C_{15}H_{15}N_3O_2$) was measured in-house to be 6.04 ppb/K in DMSO.[29] This compound acts as a reference wherein it is clear that only intermolecular hydrogen bonds are present in the solution of this compound.

4. CONCLUSION

Extensive DFT/TD-DFT calculations have been performed on coumarin 343 in order to comprehend its molecular aggregation mechanisms in solution. Two types of aggregates in nonpolar solvents have been identified: dimers and high-order J-aggregates. Their respective formation mechanisms are proposed in order to rationalize the distinct UV−vis absorption profiles of this coumarin, which depend upon solution preparation methods, even if the solutions are of the same solute, the same solvent, the same temperature and the same (apparent) concentration. However, as solvent polarity rises, dimers are shown to become less stable relative to monomers and high-order aggregates of coumarin 343. It has also been demonstrated that the molecular aggregation of this compound is largely responsible for many inconsistent λ_{max}^{abs} values reported in the literature.

Furthermore, the traditional view on the most stable conformation of coumarin 343 in hydrogen-bond accepting (HBA) solvents is challenged. Previous studies have suggested that the −COOH group of this coumarin forms an intramolecular hydrogen bond both in vacuo and in solution. However, we have argued, using both DFT calculations and ^{1}H NMR spectroscopy experiments, that by "opening up" this bond, coumarin 343 has more extensive interactions with HBA solvents via intermolecular hydrogen bonds and becomes more stable.

This study leads to a deeper understanding of solvent effects on the molecular aggregation and complex formation mechanisms of coumarin 343. It demonstrates the importance of specific solvent effects in determining the most stable molecular conformations of coumarin 343, and provides an important foundation for the formulation of antiaggregation strategies for coumarin 343. Such strategies will prospect the molecular engineering of applicability of this dye to optoelectronic device technology.

AUTHOR INFORMATION

Corresponding Author

*E-mail: jmc61@cam.ac.uk. Tel: +44 (0)1223 337470. Fax: +44 (0)1223 373536.

Notes

The authors declare no competing financial interest.

ACKNOWLEDGMENTS

The authors thank Dr. Paul Waddell from the Department of Physics, University of Cambridge, U.K., for his helpful comments on this manuscript; Dr. Roger Coulston from the Department of Chemistry, University of Cambridge, U.K., for his assistance with the NMR spectroscopic experiments; Dr. Mariano Correa from the Department of Chemistry, National University of Rio Cuarto, Argentina, for sharing their experimental details; and the EPSRC UK National Service for Computational Chemistry Software (NSCCS), based at Imperial College London, and contributions from its staff in supporting this work. X.L. is indebted to the Singapore Economic Development Board for a Clean Energy Scholarship. K.S.L. acknowledges the EPSRC for a DTA Ph.D. studentship (EP/P504120/1). J.M.C. thanks the Royal Society for a University Research Fellowship, the University of New Brunswick (UNB), Canada, for The UNB Vice-Chancellor's Research Chair and NSERC for the Discovery Grant, 355708.

REFERENCES

(1) (a) Correa, N. M.; Levinger, N. E. What Can You Learn from a Molecular Probe? New Insights on the Behavior of C343 in Homogeneous Solutions and AOT Reverse Micelles. *J. Phys. Chem. B* **2006**, *110*, 13050−13061. (b) Gutierrez, J. A.; Falcone, R. D.; Silber, J. J.; Correa, N. M. Role of the Medium on the C343 Inter/Intramolecular Hydrogen Bond Interactions. An Absorption, Emission, and ^{1}HNMR Investigation of C343 in Benzene/*n*-Heptane Mixtures. *J. Phys. Chem. A* **2010**, *114*, 7326−7330.

(2) Duarte, F. J.; Hillman, L. W. *Dye Laser Principles, with Applications*; Academic Press: San Diego, CA, 1990.

(3) (a) Hara, K. Dye-sensitized Nanocrystalline TiO_2 Solar Cells Based on Novel Coumarin Dyes. *Sol. Energy Mater. Sol. Cells* **2003**, *77*, 89−103. (b) Hara, K.; Sato, T.; Katoh, R.; Furube, A.; Ohga, Y.; Shinpo, A.; Suga, S.; Sayama, K.; Sugihara, H.; Arakawa, H. Molecular Design of Coumarin Dyes for Efficient Dye-Sensitized Solar Cells. *J. Phys. Chem. B* **2002**, *107*, 597−606.

(4) Weber, M. J. *Handbook of Lasers*; CRC Press: Boca Raton, FL, 2001.
(5) Hao, E.; Anderson, N. A.; Asbury, J. B.; Lian, T. Effect of Trap States on Interfacial Electron Transfer between Molecular Absorbates and Semiconductor Nanoparticles. *J. Phys. Chem. B* **2002**, *106*, 10191−10198.
(6) Hara, K.; Kurashige, M.; Dan-oh, Y.; Kasada, C.; Shinpo, A.; Suga, S.; Sayama, K.; Arakawa, H. Design of New Coumarin Dyes Having Thiophene Moieties for Highly Efficient Organic-dye-sensitized Solar Cells. *New J. Chem.* **2003**, *27*, 783−785.
(7) Reynolds, G. A.; Drexhage, K. H. New Coumarin Dyes with Rigidized Structure for Flashlamp-pumped Dye Lasers. *Opt. Commun.* **1975**, *13*, 222−225.
(8) Baussard, J.-F.; Habib-Jiwan, J.-L.; Laschewsky, A. Enhanced Förster Resonance Energy Transfer in Electrostatically Self-Assembled Multilayer Films Made from New Fluorescently Labeled Polycations. *Langmuir* **2003**, *19*, 7963−7969.
(9) (a) Cave, R. J.; Castner, E. W., Jr. Time-dependent Density Functional Theory Investigation of the Ground and Excited States of Coumarins 102, 152, 153, and 343. *J. Phys. Chem. A* **2002**, *106*, 12117−12123. (b) Wu, W.; Cao, Z.; Zhao, Y. Theoretical Studies on Absorption, Emission, and Resonance Raman Spectra of Coumarin 343 Isomers. *J. Chem. Phys.* **2012**, *136*, 114305. (c) Preat, J.; Jacquemin, D.; Wathelet, V.; André, J. M.; Perpète, E. A. TD-DFT Investigation of the UV Spectra of Pyranone Derivatives. *J. Phys. Chem. A* **2006**, *110*, 8144−8150. (d) Cave, R. J.; Burke, K.; Castner, E. W., Jr Theoretical Investigation of the Ground and Excited States of Coumarin 151 and Coumarin 120. *J. Phys. Chem. A* **2002**, *106*, 9294−9305.
(10) Reichardt, C.; Welton, T. *Solvents and Solvent Effects in Organic Chemistry*; Wiley-VCH: Weinheim, Germany, 2011.
(11) Lakowicz, J. R. *Principles of Fluorescence Spectroscopy*; Springer: New York, 2006.
(12) (a) Liu, X.; Cole, J. M.; Low, K. S. Solvent Effects on the UV−vis Absorption and Emission of Optoelectronic Coumarins: a Comparison of Three Empirical Solvatochromic Models. *J. Phys. Chem. C* **2013**, *117*, 10.1021/jp310397z. (b) Moog, R. S.; Davis, W. W.; Ostrowski, S. G.; Wilson, G. L. Solvent Effects on Electronic Transitions in Several Coumarins. *Chem. Phys. Lett.* **1999**, *299*, 265−271. (c) Moog, R. S.; Kim, D. D.; Oberle, J. J.; Ostrowski, S. G. Solvent Effects on Electronic Transitions of Highly Dipolar Dyes: a Comparison of Three Approaches. *J. Phys. Chem. A* **2004**, *108*, 9294−9301.
(13) Frisch, M. J.; et al. *Gaussian 09*; Gaussian Inc.: Wallingford, CT, 2009.
(14) (a) Stephens, P. J.; Devlin, F. J.; Chabalowski, C. F.; Frisch, M. J. Ab Initio Calculation of Vibrational Absorption and Circular Dichroism Spectra Using Density Functional Fields. *J. Phys. Chem.* **1994**, *98*, 11623−11627. (b) Becke, A. D. Density-functional Thermochemistry. III. the Role of Exact Exchange. *J. Chem. Phys.* **1993**, *98*, 5648−5652. (c) Lee, C.; Yang, W.; Parr, R. G. Development of the Colle-salvetti Correlation-energy Formula into a Functional of the Electron Density. *Phys. Rev. B* **1988**, *37*, 785−789.
(15) (a) Krishnan, R.; Binkley, J. S.; Seeger, R.; Pople, J. A. Self-consistent Molecular-orbital Methods. XX. Basis Set for Correlated Wave-functions. *J. Chem. Phys.* **1980**, *72*, 650−654. (b) McLean, A. D.; Chandler, G. S. Contracted Gaussian Basis Sets for Molecular Calculations. I. Second Row Atoms, Z= 11−18. *J. Chem. Phys.* **1980**, *72*, 5639−5648.
(16) (a) Boys, S. F.; Bernardi, F. The Calculation of Small Molecular Interactions by the Differences of Separate Total Energies. Some Procedures with Reduced Errors. *Mol. Phys.* **1970**, *19*, 553−566. (b) Simon, S.; Duran, M.; Dannenberg, J. J. How Does Basis Set Superposition Error Change the Potential Surfaces for Hydrogen-bonded Dimers? *J. Chem. Phys.* **1996**, *105*, 11024−11031.
(17) Rassolov, V. A.; Ratner, M. A.; Pople, J. A.; Redfern, P. C.; Curtiss, L. A. 6-31G* basis set for third-row atoms. *J. Comput. Chem.* **2001**, *22*, 976−984.
(18) (a) Chipman, D. M. Reaction Field Treatment of Charge Penetration. *J. Chem. Phys.* **2000**, *112*, 5558−5565. (b) Miertus, S.; Scrocco, E.; Tomasi, J. Electrostatic Interaction of a Solute with a Continuum. A Direct Utilizaion of Ab Initio Molecular Potentials for the Prevision of Solvent Effects. *Chem. Phys.* **1981**, *55*, 117−129.
(19) Würthner, F.; Kaiser, T. E.; Saha-Möller, C. R. J-Aggregates: from Serendipitous Discovery to Supramolecular Engineering of Functional Dye Materials. *Angew. Chem., Int. Ed.* **2011**, *50*, 3376−3410.
(20) Liu, X.; Cole, J. M.; Waddell, P. G.; Lin, T.-C.; McKechnie, S. The Molecular Origins of Optoelectronic Properties in Coumarins 343, 314T, 445 and 522B. *J. Phys. Chem. C* 2013, DOI:10.1021/jp400614e.
(21) (a) Kamlet, M. J.; Taft, R. The Solvatochromic Comparison Method. I. The β-Scale of Solvent Hydrogen-bond Acceptor (HBA) Basicities. *J. Am. Chem. Soc.* **1976**, *98*, 377−383. (b) Taft, R.; Kamlet, M. J. The Solvatochromic Comparison Method. 2. The α-Scale of Solvent Hydrogen-bond Donor (HBD) Acidities. *J. Am. Chem. Soc.* **1976**, *98*, 2886−2894. (c) Kamlet, M. J.; Abboud, J. L.; Taft, R. The Solvatochromic Comparison Method. 6. The π^* Scale of Solvent Polarities. *J. Am. Chem. Soc.* **1977**, *99*, 6027−6038. (d) Kamlet, M. J.; Abboud, J. L. M.; Abraham, M. H.; Taft, R. Linear Solvation Energy Relationships. 23. A Comprehensive Collection of the Solvatochromic Parameters π^*, α, and β, and Some Methods for Simplifying the Generalized Solvatochromic Equation. *J. Org. Chem.* **1983**, *48*, 2877−2887.
(22) Correa, M. Department of Chemistry, National University of Rio Cuarto, Argentina. *Personal communication*, June 2012.
(23) Silverstein, R.; Webster, F. *Spectrometric Identification of Organic Compounds*; John Wiley & Sons: New York, 2006.
(24) The solvent parameters for this mixture are estimated by taking the weighted average solvent parameters of the individual solvents in the mixture.
(25) Marcus, Y. The Properties of Organic Liquids That Are Relevant to Their Use as Solvating Solvents. *Chem. Soc. Rev.* **1993**, *22*, 409−416.
(26) Kasha, M.; Rawls, H. R.; El-Bayoumi, M. A. The Exciton Model in Molecular Spectroscopy. *Pure Appl. Chem.* **1965**, *11*, 371−392.
(27) (a) Poppe, L.; Van Halbeek, H. Nuclear Magnetic Resonance of Hydroxyl and Amido, Protons of Oligosaccharides in Aqueous Solution: Evidence for a Strong Intramolecular Hydrogen Bond in Sialic Acid Residues. *J. Am. Chem. Soc.* **1991**, *113*, 363−365. (b) Poppe, L.; Stuike-Prill, R.; Meyer, B.; Van Halbeek, H. The Solution Conformation of Sialyl-α(2→6)-lactose Studied by Modern NMR Techniques and Monte Carlo Simulations. *J. Biomol. NMR* **1992**, *2*, 109−136. (c) Besombes, S.; Utille, J. P.; Mazeau, K.; Robert, D.; Taravel, F. R. Conformational Study of a Guaiacyl β-o-4 Lignin Model Compound by NMR. Examination of Intramolecular Hydrogen Bonding Interactions and Conformational Flexibility in Solution. *Magn. Reson. Chem.* **2004**, *42*, 337−347.
(28) McGarry, P. F.; Jockusch, S.; Fujiwara, Y.; Kaprinidis, N. A.; Turro, N. J. DMSO Solvent Induced Photochemistry in Highly Photostable Compounds. the Role of Intermolecular Hydrogen Bonding. *J. Phys. Chem. A* **1997**, *101*, 764−767.
(29) Zhang, L.; Cole, J. M.; Waddell, P. G.; Low, K. S.; Liu, X. Relating Electron Donor and Carboxylic Acid Anchoring Substitution Effects in Azo Dyes to Dye-sensitized Solar Cell Performance. In preparation.